Journal of Electron Spectroscopy and Related Phenomena 229 (2018) 47–51

Contents lists available at ScienceDirect

Journal of Electron Spectroscopy and Related Phenomena

journal homepage: www.elsevier.com/locate/elspec

Electronic properties of composite iron (II, III) oxide (Fe_3O_4) carbonaceous absorber materials by electron spectroscopy

Dahlang Tahir[a,*], Sultan Ilyas[a], Bualkar Abdullah[a], Bidayatul Armynah[a], Hee Jae Kang[b]

[a] Department of Physics, Hasanuddin University, Makassar 90245, Indonesia
[b] Department of Physics, Chungbuk National University, Cheongju, 361-763, Republic of Korea

ARTICLE INFO

Keywords:
XPS
REELS
FTIR
Reflection loss
Magnetic loss

ABSTRACT

Electronic properties of composite Fe_3O_4 carbonaceous absorber materials were obtained by using X-ray photoelectron spectroscopy (XPS), reflection electron energy loss spectroscopy (REELS), and Fourier transforms infrared spectroscopy (FTIR). The bandgap of composite was increasing slightly from 2.5 eV for 10% activated carbon (AC) to 2.9 eV for 25% AC. The increase in the band-gap of the composite confirms; the bonding formation by the charge transfer complex between surface hydroxyl groups of Fe_3O_4 and carbonaceous in the form of AC particle. From the REELS, XPS, and FTIR shows effective orbital hybridization between the 2p(O), π(C) orbitals of amorphous carbon and 3d (Fe) orbital of Fe_3O_4 could lead to strong bonding formation of O-C-Fe_{1-x}-O. For all composites shows reflection loss (R) values less than -10 dB can be designed to attenuate EM wave, thus the composites in this study are very promising for new types of EM wave absorptive materials.

1. Introduction

Composites metal oxide and carbonaceous are promising materials for an absorber electromagnetics (EM) waves, heterogeneous catalysts, pharmaceutical, biomedical and cosmetic formulations, and photocatalyst applications [1–6]. Absorber applications have high attention due to environmental viability with good organic bonding chemical stability. In order to increase this physical phenomenon, an alternative material is proposed and investigated for replacement of conventional of bio-carbon and reducing magnetic properties. The basic criteria for a bio-carbon are including organic linker that will effectively stable in absorbing EM waves, chemical stability in contact with metal oxide materials, and a low density (light) [1,5]. Among many possible candidates, carbonaceous materials in the form of activated carbon (AC) are promising candidates for increasing organic linker and reducing magnetic properties of metal oxides [2,6]. Even though they have lower magnetic properties, they are relatively easy for breaking bond at surface during operation as absorber material, and hence needed for further improvement. For this reason, carbonaceous in the form of activated carbon (AC) usually amorphous solids with large internal surface areas and pore volumes have been intensively studied because of their structural properties. Furthermore, the incorporation of AC into metal oxides helps for stabilizing an amorphous metal carbonaceous structure, reducing magnetic properties, and to avoid the formation of unstable bonding at the surface of bio-metal composites. There are two main parameters for us to consider in increasing the organic bonding stability. The first parameter is the effective orbital hybridization between surface carbonaceous and metal oxide, and the second parameter is interfacial charge transfer complex formation and bonding formation between electron from carbonaceous and metal oxide. Hence, the interfacial charge transfers complex formation and bonding formation are the most fundamental properties needed in characterizing the absorber materials. In addition to the strong bonding formation is a potentially stabilizing the absorber material during operation. To get a clear insight into the structural properties for bio-metal composites, a better understanding for the chemical and electronic structure of amorphous metal carbonaceous is necessary, e.g., we need to characterize their electronic structures such as bonding formation in nanometer-scale spatial resolution.

Due to high complexion bonding at the surface of AC with Fe_3O_4, it can be utilized pore of AC as a linker for composite Fe_3O_4-AC. Despite light harvesting, the problem with surface attached organic linker is highly unstable under the operating conditions for absorber electromagnetic application and the bonding formation can be break out during absorption of EM [3,5–7].

In order to use Fe_3O_4 carbonates for absorber materials, they should have stable bonding bio-metal oxide surface complex to inhibit the stable carbonaceous bonding for absorber EM. Development of stable

* Corresponding author.
E-mail address: dtahir@fmipa.unhas.ac.id (D. Tahir).

https://doi.org/10.1016/j.elspec.2018.09.008
Received 20 July 2018; Received in revised form 22 September 2018; Accepted 22 September 2018
Available online 24 September 2018
0368-2048/

bonding between Fe_3O_4 and AC is essential in understanding stable bonding organic-inorganic metal oxide for absorber materials. So far, bonding formation and magnetic properties of Fe_3O_4 have not been experimentally investigated adequately. In the our previous work, electron spectroscopy (XPS and REELS) has been successfully used to analysis electronic properties of dielectric materials, semiconductor, metal and their oxide, transparent oxide materials, polymer, and composite metal-silicate [8–21]. Hence, we would like to investigate the bonding formation of Fe_3O_4-AC composites by using X-ray photoelectron spectroscopy, Fourier transform infra-red spectroscopy, reflection electron energy loss spectroscopy, magnetic properties by vibrating sample magnetometer (VSM), and absorption characteristic by VNA measurements.

2. Materials and methods

Iron (II, III) oxide nanopowder (Fe_3O_4) was purchased from Sigma Aldrich with particle size is 50–100 nm and trace metals basis is 97%. Activated carbon (AC) supplied from the local company PT. Cahaya Indo Abadi Indonesia with sizing an average diameter < :10 μm, purity : > 95%, surface area: > 240 m/g. PVA (Polyvinyl Alcohol) purity 99.5% was purchased from Merck.

Activated carbon (AC) was crushed into powder by using a mortar and sieved with 200 meshes. For homogeneous composites, the Fe_3O_4 was mixed with AC by Retsch MM for 30 min at frequency 10 Hz, which was controlled by X-ray fluorescence (XRF). We made 2 samples for each composition, the first sample we used to determine the minimum mixed time for producing a homogeneous composition which was measured by XRF for every 5 min. We found the total mixing times for all samples shows homogeneous composition is 25 min. The second sample is used for characterization and analysis in this study by mixing directly for 30 min. The final mass of each sample is 15 g in composite that consists of 10%, 15%, 20%, and 25% of AC.

For XPS and REELS spectra were obtained by using the VG ESCALAB 210 which was described in detail in our previous paper [8–11,13–22]. Spectra were measured using Mg source with the pass energy of 20 eV. The incident and take off angles of electrons were 55° and 0° from the surface normal, respectively. REELS were measured with the primary electron energy of 1.5 keV for excitation. The full width at half maximum (FWHM) of the elastic peak was 0.8 eV with the constant analyzer pass energy of 20 eV.

Fourier Transforms Infrared (FTIR) spectroscopy was carried out on IRPrestige-21 FT-IR spectrometer (Shimadzu Corp) equipped with a bright ceramic light source, a KBr beamsplitter, and a deuterated triglycine sulfate doped with L-alanine (DLATGS) detector. The measurements of the sample were collected over the range of 4000-600 cm^{-1} and 16 co-added scans. All spectra of FTIR were in Transmittance units. For magnetic studies was performed by a vibrating sample magnetometer (Oxford Instruments, VSM 1.2 H).

For Electromagnetic wave absorber performance, the samples should be in the pellet form and was measured by using Vector Network Analyzer (VNA) (Rohde & Schwarz. ZVHB) with the frequency ranges from 2,5 GHz to 8 GHz. The samples (powder form) were added 5 mL in 2% concentration of PVA for each sample and poured into the beaker. Stirred samples for 30 min at 50 °C to obtain slurry form. The samples were pellet with the thickness was varied; 2 mm, 3 mm, and 4 mm by using hydraulic compactor at a pressure of 50 kPa then it was cooled naturally for 5 - 7 min. Samples were annealed in a furnace at 80 °C for 5 h.

3. Results and discussion

Fig. 1a shows the Fe 2*p* photoelectron core-level spectra for Fe_3O_4 and composite materials. One of Fe 2*d* spectra is characteristic of fully oxidized state of Fe^{2+} and Fe^{3+} for Fe_3O_4 (alternative expressed $FeO.Fe_2O_3$). The binding energies of Fe $2p_{1/2}$ and Fe $2p_{3/2}$ peaks has been reported by many researcher and the value similar with were measured in this study at 724.1 eV and 710.6 eV, respectively. Two peaks (Fe $2p_{1/2}$ and Fe $2p_{3/2}$) have the spin-orbital splitting (BE Fe $2p_{1/2}$ - BE Fe $2p_{3/2}$) is 13.5 eV which is similar reported in Ref. [1,3,21]. For composites, the binding energy of Fe 2*p* qualitatively shows the same information with the binding energy of Fe_3O_4 even the contents of AC increase up to 25% in composites. It's indicated that the Fe_3O_4 has a strong effect in the composites.

Fig. 1b shows REELS spectra for AC, Fe_3O_4, and composites. From the low energy loss spectrum, the band gap is defined as the intercept of the background level indicated by the horizontal line with the maximum negative slope near the edge values (as can be seen in Fig. 1b for 25% AC, the arrow denotes the band gap energy). The method was described in our previous paper [8–11,13–22]. We found a band gap value for AC is 4.5 eV, Fe_3O_4 is 2.4 eV and composites are slightly increased from 2.5 eV for 10% AC to 2.9 eV for 25% AC. In spite of the addition of AC elements in Fe_3O_4 within certain range, composites band gap values changed slightly due to the high bandgap of AC, similar reported in Ref [2,6,22]. For Fe_3O_4 magnetic oxide materials, the loss peak position for the electrons traveling in the solid appear at 8, 24, and 58 eV A peak at 8 eV shows strong peak may correspond to excitation of d electrons 2 eV below E_F to state 5.5 above E_F as reported in Ref. [15] for Pd. Peak around 24 eV away from the elastic center shows broad peak correspond to bulk plasmon. Small peak for composites appears at 58 eV mainly originated from Fe_3O_4 magnetic oxide which correspond to excitation of Fe *3p* electron with binding energy 53 eV to unoccupied state above EF as reported in Ref.[15] for Fe and Pd. For AC, peak around 8 eV is typical for the π plasmon (surface plasmon) for polymeric materials as reported in Ref. [10] correspond to collective excitation at surface area. For the Fe_3O_4-rich carbonate, the surface plasmon peak at about 8 eV takes advantage of the intensity relative to the contribution from Fe_3O_4. The REELS spectrum for Fe_3O_4 shows a broad peak at 24 eV correspond to the combination of the σ + π plasmon (bulk plasmon) and 2p of O electrons as reported in Ref. [10,11] and the shoulder peak at 58 eV correspond to excitation of Fe 3p electrons. The width at the onset of the loss peak for carbonates is the widest.

Band gap also defined as the energy difference between the top of the valence band and the bottom of the conduction band. The band gap of composites in this study is dependent of carbonaceous content in composites up to 25% AC. The band gap of Fe_3O_4 can be tuned by changing the concentration of AC as organic linker. The increase in the band-gap of bio-metal oxide composite confirm; the strong bonding formation by the interfacial charge transfer complex between surface hydroxyl groups of Fe_3O_4 and carbonaceous (AC) particle (It was confirmed by FT-IR spectra (see Fig. 4)). This indicated the effective orbital hybridization between the π(C) orbitals of amorphous carbon from AC and 3d (Fe) orbital of Fe_3O_4 and 2p (O) from both of AC and Fe_3O_4 resulting strong bonding formation of O—C—Fe_{1-x}-O.

Fig. 2 shows the O 1*s* and C 1*s* core level spectra for AC, Fe_3O_4 and nano-composite. For AC, the O 1*s* core level spectra shows peak formation C—O, and C—OH bonding located at 531.21 eV and 532.99 eV, respectively. The O 1*s* core level spectra for Fe_3O_4 shows bonding formation Fe—O, Fe—O—C, and Fe—OH located at 52,949 eV, 531.01 eV, and 532.60 eV, respectively. For composites shows the peak for C—O and C—OH are located at the same position but the intensity increase with increasing the amount of AC in composites probably due to the influence of Fe^{4+} in the hydroxide (Fe—OH and C—OH) matrix. The O 1*s* chemical bonding formation in composites depends on the number of second-nearest neighbor Fe or C atoms. From the XPS information, the binary deposit is oxide, denoted as O-C-Fe_{1-x}O· By investigating the chemical bonding of O 1*s*, C 1*s* core level spectra using XPS, the Fe_3O_4 and AC composites formation was confirmed from XPS and REELS spectra.

Carbonaceous molecules and Fe_3O_4 chemical bonding formation was analyzed by FT-IR spectroscopy. The FT-IR spectra of pure AC, Fe_3O_4, and bio-metal oxide composites are displayed in Fig. 3. As

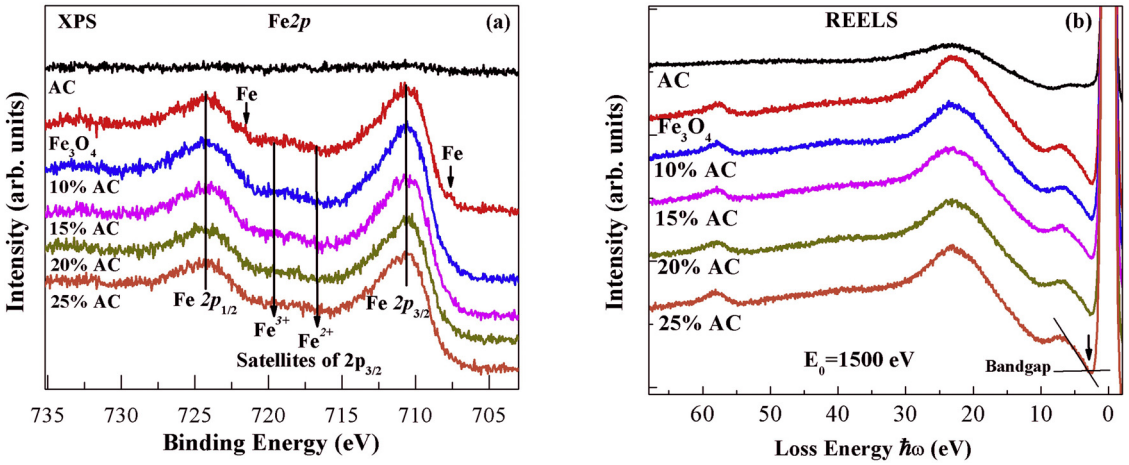

Fig. 1. (a). Fe *3d* core level photoelectron spectra for Fe_3O_4 and composite Fe_3O_4- AC (activated carbon) (10% AC, 15% AC, 20% AC, and 25% AC). (b). Reflection electron energy loss spectra for Fe_3O_4 and composite Fe_3O_4-AC (activated carbon) (10% AC, 15% AC, 20% AC, and 25% AC) at primary energy 1500 eV.

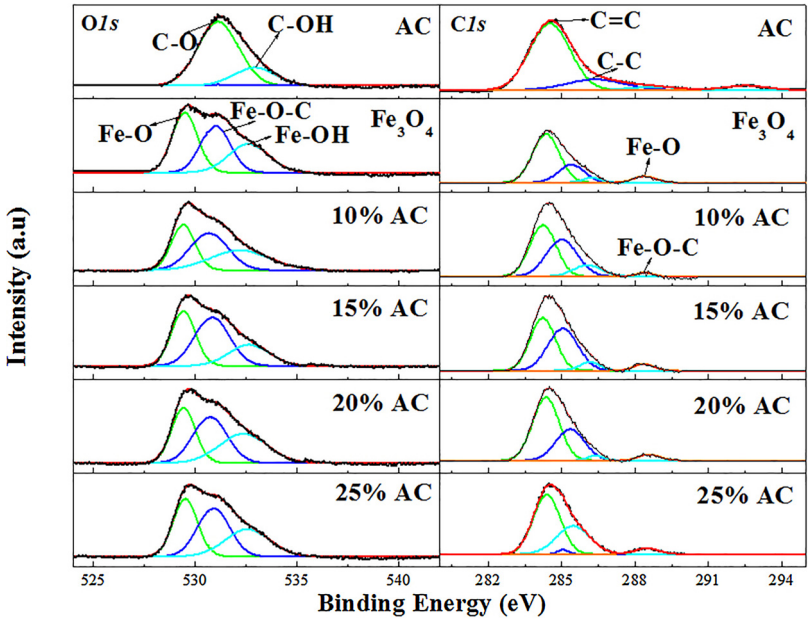

Fig. 2. O *1 s* and C *1 s* core level photoelectron spectra for Fe_3O_4 and composite Fe_3O_4-AC (activated carbon) (10% AC, 15% AC, 20% AC, and 25% AC).

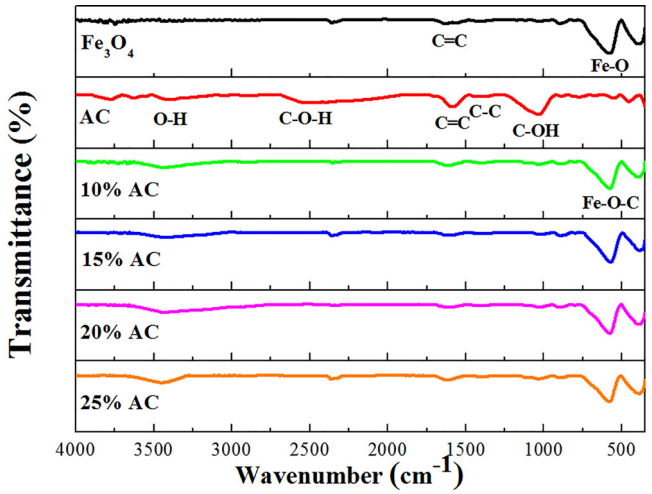

Fig. 3. Fourier transform infrared spectra for Fe_3O_4 and composite Fe_3O_4-AC (activated carbon) (10% AC, 15% AC, 20% AC, and 25% AC).

Table 1
Magnetic properties for AC, Fe_3O_4, and composite Fe_3O_4-AC (activated carbon) (10% AC, 15% AC, 20% AC, and 25% AC) determined from the Fig. 4a.

Samples	H_C (± 0.05 Oe)	M_R (± 0.05 emu/g)	M_S (± 0.05 emu/g)
AC	225.84	0.11	0.44
Fe_3O_4	251.72	21.452	93.688
10 % AC	250.30	18.193	77.277
15 % AC	245.83	16.255	68.689
20 % AC	236.38	16.179	67.640
25 % AC	226.93	15.506	62.247

shown in Fig. 3, the characteristic peaks of carbonaceous are as follows: bending vibrations C—OH appeared at 1049 cm^{-1} and C=C stretching vibrations appeared at 1586 cm^{-1}. Moreover, FT-IR spectra for composites shows existing peak of C=C cm^{-1} with normal stretching and bending vibration of carbonaceous (AC) molecules [2,6,23,24]. It is clearly demonstrated that the pore of AC molecules strongly bonding with metal oxide and it forms the stable bonding carbonaceous metal oxide. However, the peak appeared at in the range of 500–700 cm^{-1} mainly attributed for Fe—O—C bonding between Fe_3O_4 and

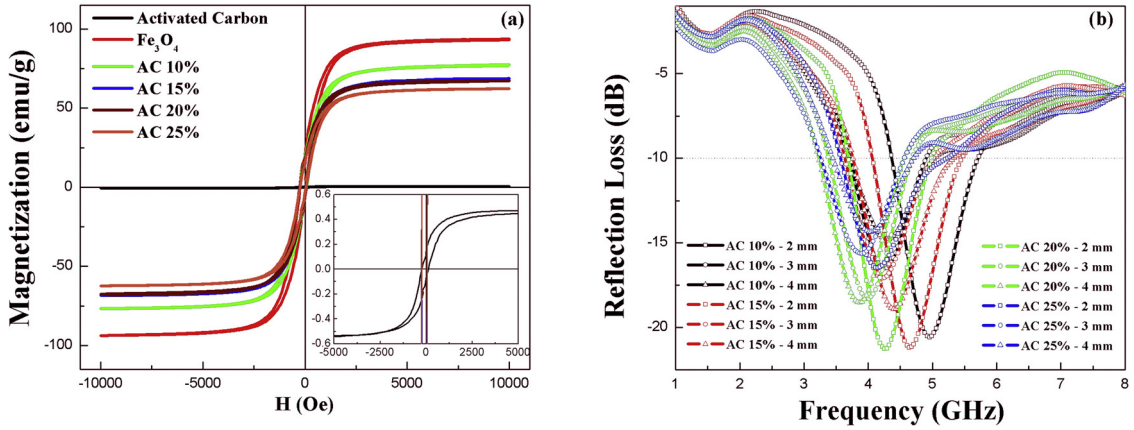

Fig. 4. (a). Magnetic properties for Fe_3O_4 and composite Fe_3O_4-AC (activated carbon) (10% AC, 15% AC, 20% AC, and 25% AC). (b). Reflection loss properties for composite Fe_3O_4-AC (activated carbon) (10% AC, 15% AC, 20% AC, and 25% AC).

Table 2
Reflection Loss (RL) properties for AC, Fe_3O_4, and composite Fe_3O_4-AC (activated carbon) (10% AC, 15% AC, 20% AC, and 25% AC) determined from the Fig. 4b.

Sample	Thickness (mm)	RL (dB)	Frequency (Hz)	Bandwidth
AC 10%	2	−20.56	4.96	1.24
	3	−16.52	4.26	1.09
	4	−14.77	4.29	1.14
AC 15%	2	−21.18	4.64	1.28
	3	−17.88	4.22	1.21
	4	−18.90	4.40	1.35
AC 20%	2	−21.26	4.26	1.21
	3	−18.29	3.98	1.23
	4	−18.52	3.87	1.26
AC 25%	2	−16.47	4.15	1.43
	3	−15.63	3.90	1.23
	4	−14.34	4.04	1.17

carbonaceous molecules. These observations confirmed that the Fe_3O_4 was strongly deposited in the pore of AC. The peaks appeared at 3438 and 2508 cm^{-1} is related to the O—H ring vibration and C—O—H bond, respectively. The very small peak at around 1400 cm^{-1} is related to C—C bond vibration [23,24]. This C—C bond vibration peak confirms that formation of the carbonaceous structure of composites. Similar C—C bond vibration was reported in Ref [24] for polymeric materials.

It is interesting to note that the bonding formation can be controlled via the maximizing the functional of the pore and concentration of AC as organic linker. As increasing the AC concentration from 10% to 25 wt % in the composites, the effective orbital's mixing and the optical band gap energy also increase.

The magnetic properties of Fe_3O_4-AC bio-metal composite materials were investigated at room temperature using a vibrating sample magnetometer with an applied field of -10 kOe < H < 10 kOe. Fig. 4a shows the hysteresis loops of the samples, Coercivity and saturation magnetization values for all samples are listed in Table 1. The coercivity of Fe_3O_4-AC composite materials decreased with the increasing the amount of the carbonaceous particles in the composite. The dependence of the saturation magnetization of Fe_3O_4-AC composite materials are shown in Table 1. The saturation magnetization values of the materials are 77.277, 68.689, 67.640, and 62.247 emu/g with the increasing the amount of AC in composites. In this present study, we found that bonding formation of metal oxides on AC via utilizing the pore can effectively increase the stability bonding formation of composites material. The resultant bonding formation Fe_3O_4 on carbonaceous material exhibits reduced magnetic properties and enhanced absorption (reflection loss). The stable bonding character of Fe_3O_4 in carbonaceous via pore of AC may find different applications in many other fields.

Fig. 4b shows the reflection loss of the composite for sample thickness was varied from 2 to 4 mm. It indicates that the maximum reflection loss reaches 21.26 dB at 4.26 GHz for the absorber whose thickness is 2 mm, for more details see Table 2. Bandwidth frequency corresponding to the reflector loss at -10 dB increased from 1.3 to 2.2 GHz [1,25,26]. AC could effectively improve the electromagnetic waves absorbing properties of the composites at the frequency range of 3.8 GHz – 4.9 GHz. The effect of thickness of composites to the electromagnetic wave absorption properties in this study can be seen clearly in Table 2. Reflection loss (R) values less than -10 dB can be designed to attenuate EM wave, thus the bio-metal composites in this study are very promising for new types of EM wave absorber materials [25,26]. The reflection loss of Fe_3O_4-AC composite is less than -10 dB, which is attributed to that the dielectric loss is significantly higher than it is the magnetic loss [25,26] The stable bonding formation of Fe_3O_4 in carbonaceous via pore of AC exhibits enhanced absorption (reflection loss) and reduced magnetic properties.

4. Conclusions

In summary, we investigated the electronic structures and chemical states for Fe_3O_4 carbonates to find suitable absorber materials with stable bonding via REELS, FTIR, and XPS analysis. The investigation provided a useful guideline for the selection of an alternative replacement for carbonaceous materials. The results showed that the stable bonding state and the band gap increase slightly with increasing amount of AC contents in Fe_3O_4 carbonaceous composite.

Acknowledgments

This work was supported by the PBK (Penelitian Berbasis Kompetensi) Grant: 1625/UN4.21/PL.00.00/2018 funded by the Indonesian Government (Ristek-Dikti) and KLN Grant: 3083/UN4.1.2/PL.00.00/2018 funded by Hasanuddin University, Makassar Indonesia.

References

[1] Yingqing Zhan, Rui Zhao, Yajie Lei, Fanbin Meng, Jiachun Zhong, Xiaobo Liu, A novel carbon nanotubes/Fe_3O_4 inorganic hybrid material: synthesis, Characterization and Microwave Electromagnetic Properties, J. Magn. Magn. Mater. 323 (2011) 1006–1010.
[2] Dae-Won Kim, Kyong-Yop Rhee, Soo-Jin Park, Synthesis of activated carbon nanotube/copper oxide composites and their electrochemical performance, J. Alloys. Compd. 530 (2012) 6–10.
[3] Zhonghua Xu, Shulin Gu, Shimin Huang, Kun Tang, Jiandong Ye, Shunming Zhu, Mingxiang Xu, Youdou Zheng, Structure and properties of Fe_3O_4 films grown on ZnO template via metal organic chemical vapor deposition, J. Magn. Magn. Mater. 385 (2015) 257–264.

[4] R. Murillo-Ortiz, M. Mirabal-Garcia, J.M. Martınez-Huerta, J.G. Cabal Velarde, I.E. Castaneda-Robles, A. Lobo-Guerrero, Analysis of the magnetic properties in hard-magnetic nanofibers composite, J. Appl. Phys. 123 (2018) 105108.
[5] Ing Kong, SahrimHj Ahmad, MustaffaHj Abdullah, David Hui, Ahmad Nazlim Yusoff, Dwi Puryanti, Magnetic and microwave absorbing properties of magnetite–thermoplastic natural rubber nanocomposites, J. Magn. Magn. Mater. 322 (2010) 3401–3409.
[6] Chien-Hung Lien, Chi-Chang Hu, Chun-Tsung Hsu, David Shan-Hill Wong, High-performance asymmetric supercapacitor consisting of Ni–Co–Cu oxy-hydroxide nanosheets and activated carbon, Electrochem. Commun. 34 (2013) 323–326.
[7] Apurba Ray, Atanu Roy, Sayan De, Souvik Chatterjee, Sachindranath Das, Frequency and temperature dependent dielectric properties of TiO_2-V_2O_5 nanocomposites, J. Appl. Phys. 123 (2018) 104102.
[8] D. Tahir, E.K. Lee, S.K. Oh, T.T. Tham, H.J. Kang, H. Jin, S. Heo, J.C. Park, J.G. Chung, J.C. Lee, Band alignment of atomic layer deposited $(ZrO_2)_x(SiO_2)_{1-x}$ gate dielectrics on Si (100), Appl. Phys. Lett. 94 (2009) 212902.
[9] D. Tahir, E.K. Lee, S.K. Oh, H.J. Kang, S. Heo, J.G. Chung, J.C. Lee, S. Tougaard, Dielectrics and optical properties of Zr silicate thin films grown on Si (100) by atomic layer deposition, J. Appl. Phys. 106 (2009) 084108.
[10] D. Tahir, S. Tougaard, Electronic and optical properties of selected polymers studied by reflection energy energy loss spectroscopy, J. Appl. Phys. 111 (2012) 054101.
[11] D. Tahir, S. Tougaard, Electronic and optical properties of Cu, CuO and Cu_2O studied by electron spectroscopy, J. Phys. Condens. Matter 24 (2012) 175002.
[12] O. Romanyuk, P. Jiricek, J. Zemek, S. Tougaard, T. Paskova, Dielectric response function(0001 ¯), (101 ¯3) GaN single crystalline and disordered surface studied by reflection electron energy loss spectroscopy, J. Appl. Phys. 110 (2011) 043507.
[13] Y.S. Denny, H.C. Shin, S. Seo, S.K. Oh, H.J. Kang, D. Tahir, S. Heo, J.G. Chung, J.C. Lee, S. Tougaard, Electronic and optical properties of hafnium indium zinc oxide thin film by XPS and REELS, J. Electron Spectrosc. Relat. Phenom. 185 (2012) 18.
[14] H.C. Shin, D. Tahir, S. Seo, Y.R. Denny, S.K. Oh, H.J. Kang, S. Heo, J.G. Chung, J.C. Lee, S. Tougaard, Reflection electron energy loss spectroscopy for ultrathin gate oxide materials, Surf. Interface Anal. 44 (2012) 623.
[15] D. Tahir, J. Kraaer, S. Tougaard, Electronic and optical properties of Fe, Pd, and Ti studied by reflection electron energy loss spectroscopy, J. Appl. Phys. 115 (2014) 243508.
[16] D. Tahir, N.H. Suarga, Sari, and Yulianti, Stopping powers and inelastic mean free path of 200 eV-50 keV electrons in polymer PMMA, PE, and PVC, Appl. Radiat. Isot. 95 (2015) 59–62.
[17] D. Tahir, E.K. Lee, E.H. Choi, S.K. Oh, H.J. Kang, S. Heo, J.G. Chung, J.C. Lee, S. Tougaard, Electronic and optical properties of Al_2O_3/SiO_2 thin films grown on Si substrate, J. Phys. D Appl. Phys. 43 (2010) 255301.
[18] D. Tahir, Y.J. Cho, S.K. Oh, H.J. Kang, H. Jin, S. Heo, J.G. Park, J.C. Lee, S. Tougaard, Electronic and optical properties of La-aluminate dielectric thin films on Si (100), Surf. Interface Anal. 42 (2010) 1566–1569.
[19] D. Tahir, E.K. Lee, S.K. Oh, H.J. Kang, E.H. Lee, J.G. Chung, J.C. Lee, S. Tougaard, Electronic and optical properties of GIZO thin film grown on SiO2 substrate, Surf. Interface Anal. 42 (2010) 906–910.
[20] D. Tahir, S.K. Oh, H.J. Kang, S. Tougaard, Quantitative analysis of reflection electron energy loss spectra to determine electronic and optical properties of Fe-Ni alloy thin films, J. Electron Spectrosc. Relat. Phenom. 206 (2016) 6–18.
[21] D. Tahir, S.K. Oh, H.J. Kang, S. Tougaard, Composition Dependence of Dielectric and Optical Properties of Hf-Zr-Silicate Thin Films Grown on Si(100) by Atomic Layer Deposition, Thin Solid Films 616 (2016) 425–430.
[22] Pooja Saini, Manjri Singh, Surinder P.Singh, Ajit K.Mahapatro, Spectroscopic and electronic properties of polyallylamine functionalized graphene oxide films, Vacuum 54 (2018) 110–114.
[23] YantongLi TaoXu, Jiayu Chen, Huijun Wu, Xiaoqing Zhou, Zhengguo Zhang, Improving thermal management of electronic apparatus with paraffin (PA)/expanded graphite (EG)/graphene (GN) composite material, Appl. Therm. Eng. 140 (2018) 13–22.
[24] Ifra Marriam, Fujun Xu, Mike Tebyetekerwa, Yang Gao, Wei Liu, Xiaohua Liu, Yiping Qiu, Synergistic effect of CNT films impregnated with CNT modified epoxy solution towards boosted interfacial bonding and functional properties of the composites, Compos. Part A Appl. Sci. Manuf. 110 (2018) 1–10.
[25] Linna Dai, Shengkun Xie, Meijie Yu, Lijie Ci, Fabrication and electromagnetic properties of carbon-based Iron nitride composite, J. Magn. Magn. Mater. 466 (2018) 22–27.
[26] Bualkar Abdullah, Sultan Ilyas, Dahlang Tahir, Nanocomposites Fe/Activated Carbon/PVA for microwave absorber: synthesis and characterization, . 6 (2018), https://doi.org/10.1155/2018/9823263.